

# SPATIAL ANALYSIS ON OCCURRENCE FACTORS OF MULTIPLE SLOPE FAILURES USING TOPOGRAPHIC AND RAINFALL INDICES WITH HIGH SPATIAL RESOLUTIONS

\* Takashi Wada<sup>1</sup>, Ryo Kodani<sup>2</sup> and Hiroshi Miwa<sup>1</sup>

<sup>1</sup> Department of Social Systems and Civil Engineering, Tottori University, Japan; <sup>2</sup> Tottori City Office, Japan

\*Corresponding Author, Received: 17 Jun. 2020, Revised: 13 Jan. 2021, Accepted: 29 Jan. 2021

**ABSTRACT:** In this study, the spatial characteristics of the factors influencing the occurrence and scale of multiple slope failures in areas with smaller grid sized than the unit size for the current emergency alert system for sediment disasters in Japan were investigated by using high-resolution data for the spatial distribution of topography and rainfall. The study areas were located in southern Hiroshima Prefecture and southeastern Ehime Prefecture of Japan, where multiple slope failures occurred due to heavy rainfall in July 2018. With an increase in slope gradient, the frequency of smaller-scale slope failures increases significantly in southeastern Ehime Prefecture, whereas this tendency is not as noticeable in southern Hiroshima Prefecture. This indicates that other indices (e.g., geological feature, large total precipitation) also influence the occurrence of slope failure. A slope-facing direction is not seem to affect the occurrence of slope failure in both study areas. Total precipitation (i.e., long-term rainfall index) influence the frequency of the occurrence of slope failure in southern Hiroshima Prefecture. Whereas, maximum hourly precipitation (i.e., short-term rainfall index) relates to the occurrence of slope failure in both study areas. These indicate that the occurrence of slope failures depend on different rainfall indices in each study area. Combining the topographic indices (e.g., slope gradient) and rainfall indices (e.g., hourly precipitation, total precipitation) may lead to a highly accurate estimation of the occurrence of slope failure on a smaller grid size than the unit size for the current system.

*Keywords: Multiple slope failures, Slope gradient, Maximum hourly precipitation, Total precipitation, GIS data*

## 1. INTRODUCTION

Recently, the multiple sediment disasters, such as the disaster caused by the heavy rainfall due to the seasonal rain front and Typhoon Prapiroon in July 2018, have increased in Japan. Since the heavy rainfall occurred intensely and widely, and led to total precipitation of over 400 mm, it caused the serious sediment disasters in most part of Hiroshima and Ehime Prefectures of Japan [1, 2]. At 70% of the areas in which human lives were lost by the disaster, the emergency alert for sediment disasters was announced for local inhabitants before disaster occurrence [3]. However, this alert was not utilized enough for inhabitants resulting in the loss of many human lives at these areas. The possible reason for this is that the unit size of the current emergency alert system for sediment disasters in Japan is too large (mainly a grid of 5 km) so that local inhabitants have difficulties in perceiving an increased possibility of nearby slope failure and sediment runoff by the emergency alert. In addition, the unit size is also too large to consider the local conditions of surface topography and precipitation which may influence the occurrence of a slope failure more strongly.

Considering the above-mentioned facts, it is

necessary to establish an emergency alert system for sediment disasters on a smaller scale than that of the current system. Before a new system is implemented, it is necessary to investigate the spatial characteristics of local land factors (e.g., surface topography, geological features, land use conditions) and meteorological triggers (e.g., short- and long-term rainfall indices, wind direction), which can influence the occurrence and scale of slope failures on a smaller grid scale.

It is widely accepted that high intensity and high duration rainfall events are the most important trigger for slope failures worldwide [4, 5]. As such, in recent decades, several researchers have attempted to establish a rainfall-based alert system for sediment disasters [6]. In these systems, threshold for slope failures usually depends on the intensity and duration of rainfall events, and this is defined as a minimum intensity of rainfall for a specific duration which is needed for an occurrence of a slope failure [7]. In Japan, a rainfall-based alert system for sediment disasters uses the short-term rainfall index (e.g., hourly precipitation) and the long-term rainfall index (e.g., antecedent rainfall, several-day precipitation or soil water index) to determine the threshold for an occurrence of slope failure, that is the critical line (CL). This method is

structured by considering that mass movements of failures are driven by surface water generated by short-term rainfall, and ground water risen by long-term rainfall [8]. The Japanese alert system is common to the overseas system in terms of considering short-term and long-term rainfall indices for an occurrence of slope failure. However, the spatial resolution of these systems is low because of using the rainfall data obtained at the sparse observation points spatially. Therefore, it is difficult to investigate the local relationships between the rainfall indices and the occurrence factors influencing slope failure for small watersheds and districts. For example, the rainfall data used by the Japanese alert system is 1 km-grid analytical rainfall data by the radar automated meteorological data acquisition system (radar AMeDAS) produced by the Japan Meteorological Agency (JMA), which combines the rainfall data obtained by ground rain-gauges and microwave radars. Therefore, the unit size of the rainfall data is too large to consider the local precipitation in small watersheds and districts. In addition, in the system, the local factors such as a surface topography, a geological feature and a land use condition are not considered to determine the critical line (CL) for an occurrence of a slope failure.

Several researchers have attempted to investigate a relationship between several local factors and a slope failure using Geographic Information System (GIS) data and aerial photographs. Yamagishi *et al.* [9] investigated the spatial characteristics of the surface topography and the geological feature at the slope failures in the Izumozaki area in Niigata Prefecture of Japan by using GIS data and aerial photographs. They investigated these characteristics at the slope failures caused by the heavy rainfalls in July 2004 and other past rainfalls. The results indicated that the spatial density of slope failures increased more as slope gradients increased, and the density in the sandstone area was slightly higher than that in the mudstone area. Iwahashi *et al.* [10] and Tanouchi *et al.* [11] investigated the spatial characteristics of the long-term rainfall indices (e.g., total precipitation, daily precipitation) and local land factors in the areas with multiple slope failures in Japan by using GIS data and aerial photographs. Their results indicated that the occurrence of slope failure and a slope gradient had a positive correlation as reported by Yamagishi *et al.* However, the occurrences of slope failures and slope facing direction was not remarkable. Their results also indicated that the occurrence of slope failure and long-term rainfall indices had clearly positive correlations. Kuramoto *et al.* [12] proposed the CL considering the high potential area for the local factors with a positive correlation to an occurrence of slope failure. In addition, the validity of their proposed CL was

estimated by comparing the predictive rates by their proposed CL and the conventional CL for the past multiple slope failures. As a result, the predictive rate by their proposed CL was over 10% higher than that by the conventional CL. However, since this study used the rainfall data obtained by only the ground rain-gauges which were sparse spatially, the space resolution of the rainfall data was low, and the local precipitation were not considered in this study. Therefore, it is necessary to use the rainfall data with higher spatial resolution, in order to investigate the relationship of rainfall indices and an occurrence of slope failure.

Herein, in this study, the spatial characteristics of the factors influencing the occurrence and scale of multiple slope failures in areas with smaller grid sized than the unit size for the topographic and rainfall data used in the previous studies or the current alert system were investigated. For this study, the 10-m grid Digital Elevation Model (DEM) data provided by the Geospatial Information Authority of Japan and the 250-m grid rainfall data from the extended radar information network (XRAIN) in Japan were utilized. These data were converted to the 15-m grid DEM data and the 350-m grid rainfall data by averaging spatially these data.

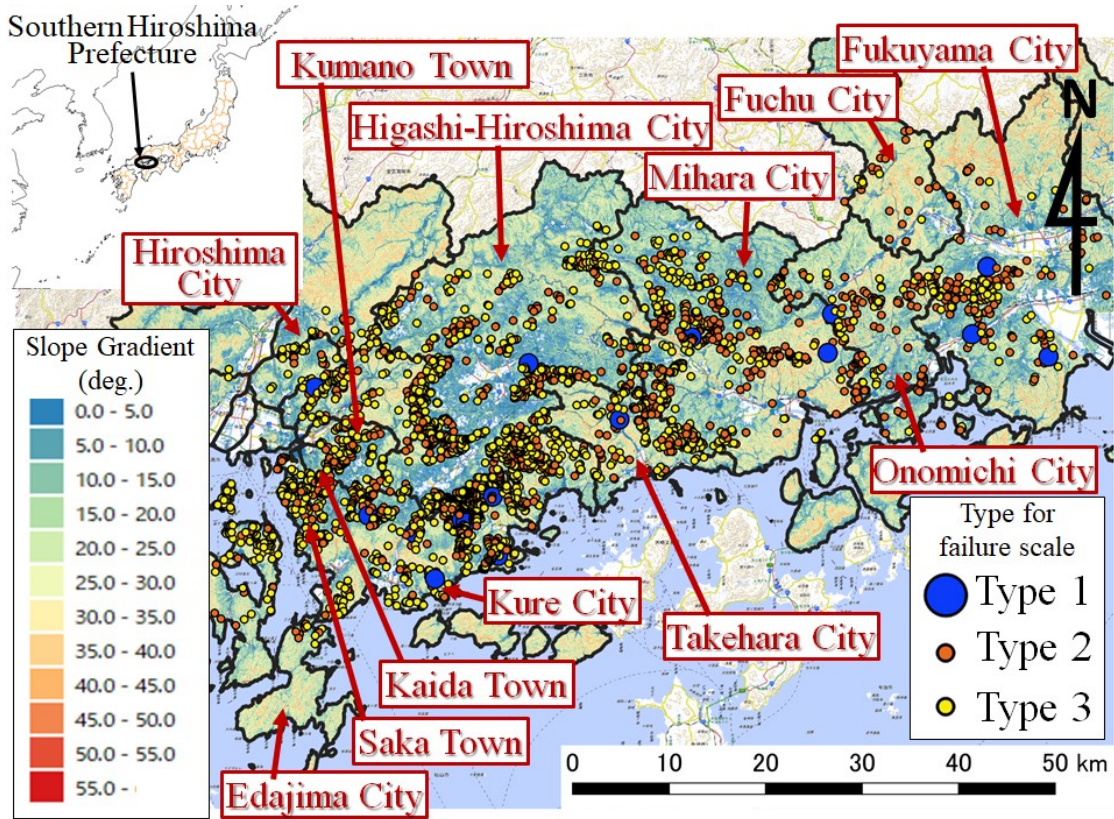
## 2. STUDY AREA AND METHODS

### 2.1 Study Area Locations

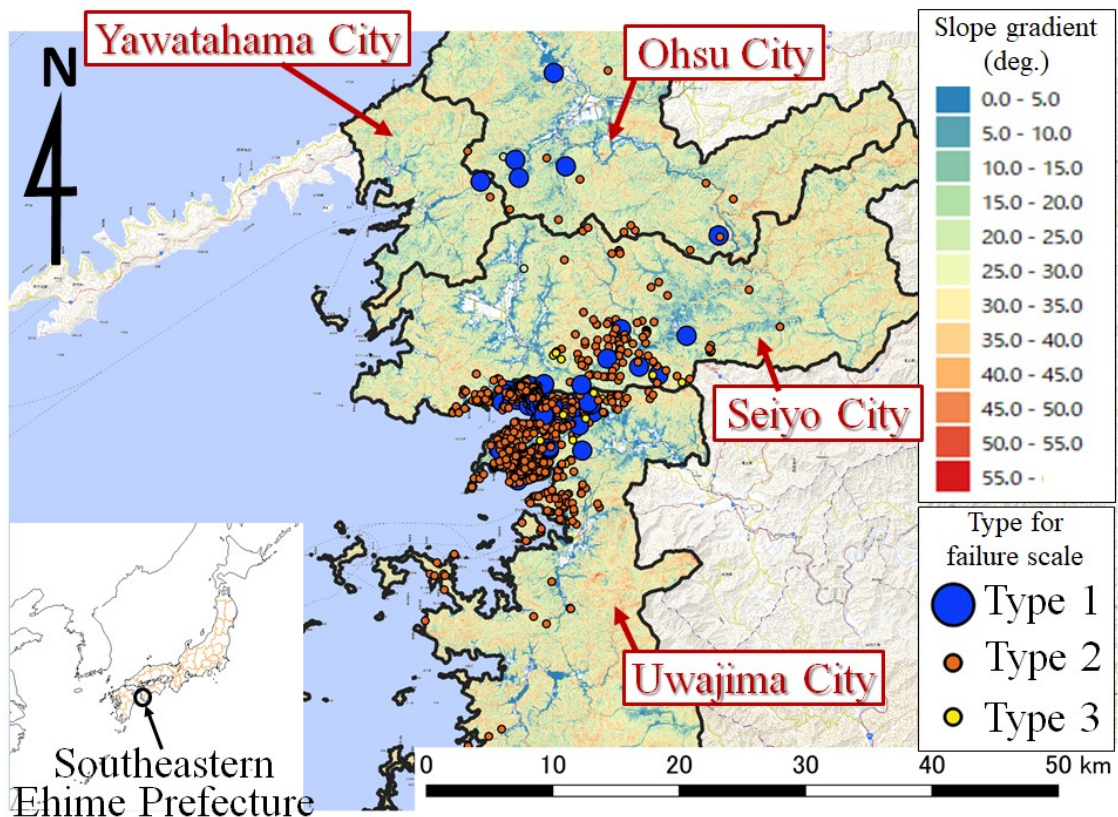
Southern Hiroshima Prefecture and southeastern Ehime Prefecture are selected as study areas. These areas are characterized by multiple slope failures that occurred by the heavy rainfall in July 2018 and led to the serious sediment disasters with many human damages. Fig. 1 shows the spatial distribution of slope failures obtained by their location from the Geospatial Information Authority of Japan and slope gradients calculated by the 15-m grid DEM data in both study areas. The slope failures were classified using the methodology described below.

### 2.2 Classification of Slope Failures

The slope failures surveyed by Sasahara *et al.* [2] (a total of 73 failures) were classified into three scale types: large-scale failure (Type 1), small-scale failure (Type 2), and erosion of a mountain stream bed (Type 3). Table 1 shows a comparison of the field survey results with the estimated results obtained using the aerial photographs by the Geospatial Information Authority of Japan for each scale type of slope failure. The slope failures classification was based on the estimated failure volume, that is, a failure with over 1,000 m<sup>3</sup> of the volume was classified as Type 1, a failure with under 1,000 m<sup>3</sup> of the volume was classified as



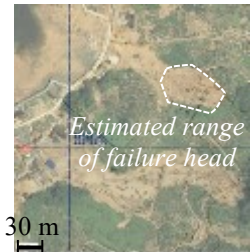
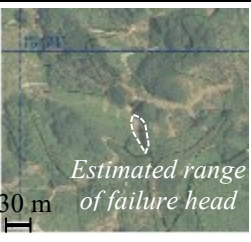
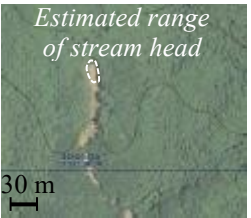
(a) Southern Hiroshima Prefecture



(b) Southeastern Ehime Prefecture

Fig.1 Spatial distribution of various slope failures caused by the heavy rainfall in July 2018 in two study areas.

Table 1 An example of a comparison of the field survey results with the aerial photograph results for each slope failure scale type in southeastern Ehime Prefecture, Japan.

Scale type of slope failure	Field survey results by Sasahara <i>et al.</i> [2]	Estimated results by the aerial photographs after the disaster
Type 1 Large scale failure	<ul style="list-style-type: none"> <li>·Failure depth; About 7.8 m</li> <li>·Failure width; About 45 m</li> <li>·Length of failure surface; About 75.5 m</li> <li>·Failure volume; About 26500 m<sup>3</sup></li> </ul> 	<ul style="list-style-type: none"> <li>·Failure head area; About 2200 m<sup>2</sup></li> </ul> 
Type 2 Small scale failure	<ul style="list-style-type: none"> <li>·Failure depth; About 1.5 m</li> <li>·Failure width; About 5 m</li> <li>·Length of failure surface; About 40 m</li> <li>·Failure volume; About 300 m<sup>3</sup></li> </ul> 	<ul style="list-style-type: none"> <li>·Failure head area; About 100 m<sup>2</sup></li> </ul> 
Type 3 Erosion of mountain stream bed	<ul style="list-style-type: none"> <li>·Erosion depth; About 2.5 m</li> </ul> 	<ul style="list-style-type: none"> <li>·Failure head area; About 80 m<sup>2</sup></li> </ul> 

Type 2, and a sediment runoff with a negligible failure area at its upstream end was classified as Type 3. By investigating the scale and area of slope failure using the aerial photographs, it was estimated that they were positively correlated. On basis of the investigating results, the areas of slope failures of Types 1, 2 and 3 were defined as over 1,000 m<sup>2</sup>, 100–1,000 m<sup>2</sup> and under 100 m<sup>2</sup>, respectively. The other slope failures were classified into three scale types with no field survey on basis of their failure areas estimated by the aerial photographs in both study areas.

Fig. 1 shows the spatial distribution of all slope failure scale types in both study areas based on the classification method described above. Fig. 2 shows the number and percentage of slope failures for each scale type and study area. The failures of Type 3 were almost absent in southeastern Ehime Prefecture, whereas they were founded in abundance in southern Hiroshima Prefecture. The percentage of Type 1 failures to all other types of failures was higher in southeastern Ehime Prefecture than in southern Hiroshima Prefecture. These results indicate that some scale type of slope failures is predominant in some regions and almost absent in other regions, despite being triggered by the same heavy rainfall. One possible reason for this is that their local land factors are different. As such,

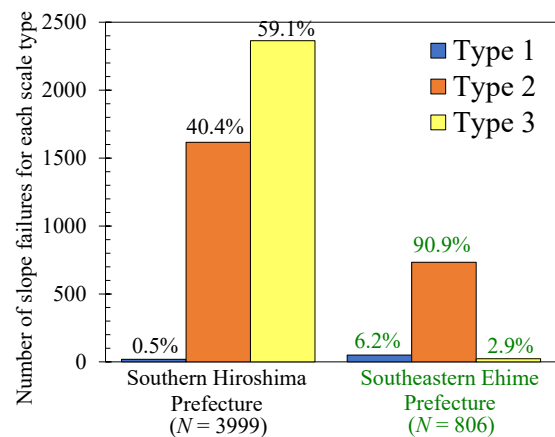


Fig. 2 Number and percentage of slope failures per each slope failure scale type.

comparing the spatial characteristics of topographic and rainfall indices, which influence the occurrence of these slope failures, between the study areas is necessary. Herein, in this study, the topographic indices are the slope gradient and slope-facing direction. The rainfall indices are the total precipitation and maximum hourly precipitation. Geological features, land use conditions and wind directions are not considered because it was difficult to compare their influence on the

occurrence of slope failures between two study areas by great difference between the characteristics of these factors in these areas.

In order to investigate the effect of these indices on slope failure, considering their appearance frequencies in the study areas, the spatial frequency of slope failures for a factor ( $F$ ) is defined by using the following equation:

$$F = \frac{\sum A_f}{\sum A} \quad (1)$$

where,  $\sum A_f$  is the total area of the target grids including slope failures;  $\sum A$  is the total area of the target grids, including all of the municipalities where the slope failures occurred in July 2018.  $F_{gr}$ ,  $F_{di}$ ,  $F_{\varphi}$  and  $F_{hp}$  are the spatial frequencies of slope failure for the slope gradient, slope-facing direction, total precipitation and maximum hourly precipitation, respectively.

### 3. RESULTS AND DISCUSSION

#### 3.1 Occurrence and Scale of Slope Failures VS. Topographic Indices

Fig. 3 shows the spatial frequency of slope failure for slope gradient  $F_{gr}$  for each slope failure scale type based on the 15-m grid-sized area. As slope gradient increases, the frequency of Type 2 and 3 increase significantly in southeastern Ehime Prefecture, whereas this tendency is not remarkable in southern Hiroshima Prefecture. This indicates that other indices, such as the geological feature (strongly weathered granite) and large total precipitation, influence the occurrence of slope failure in southern Hiroshima Prefecture. In both study areas, the frequency of Type 1 on mild slope gradients ( $< 30$  degree) is almost equal as the frequency on steep slope gradients ( $\geq 30$  degree). The reason for this is that the wide ranges of Type 1 expand to mild slopes closer to the mountain ridges. Accordingly, a slope gradient to an occurrence of slope failure is not necessarily to positively correlate because this relationship is likely influenced by other factors (e.g., geological features, total precipitation). Therefore, it is necessarily to investigate on the spatial characteristics of the combined indices of local land factors and meteorological triggers, which influence the occurrence and scale of slope failures. This investigation results are reported in the section 3.3.

Fig. 4 shows the spatial frequency of slope failure for slope-facing direction  $F_{di}$  for each slope failure scale type based on the 15-m grid-sized area.  $F_{di}$  for all slope failure scale types are almost equal and the remarkable difference of  $F_{di}$  for each scale type is not seen in each study area. This indicates that the occurrence of slope failure is unrelated to a

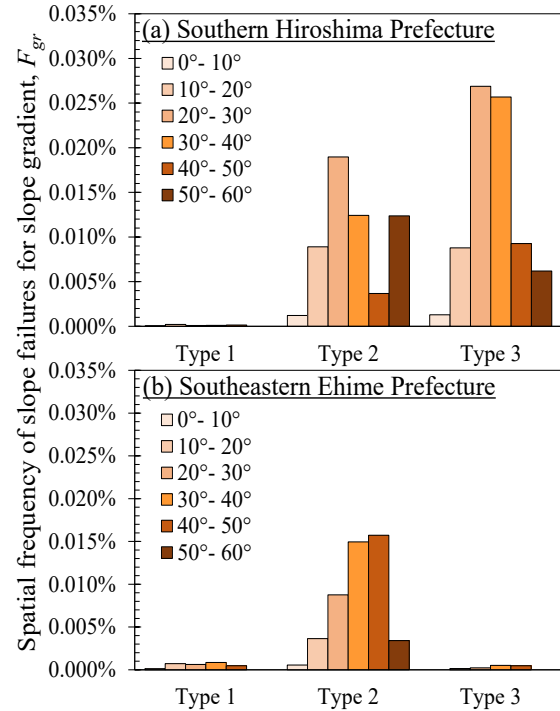


Fig. 3 Spatial frequency of slope failures for slope gradient ( $F_{gr}$ ) for each slope failure scale type based on the 15-m grid-sized area.

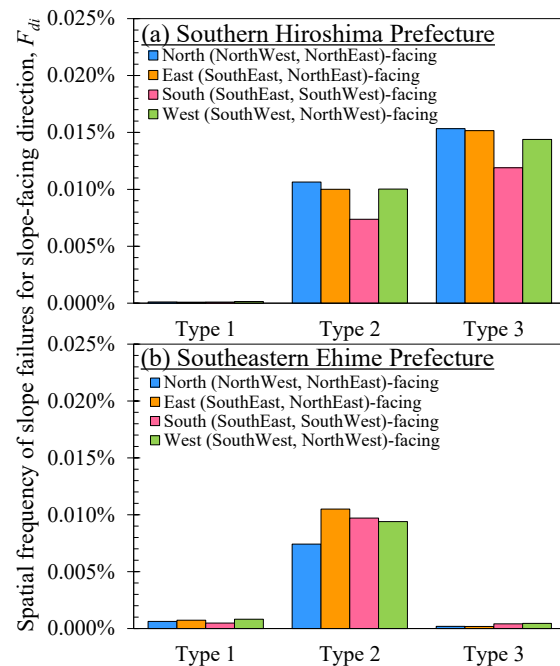


Fig. 4 Spatial frequency of slope failures for slope-facing direction ( $F_{di}$ ) for each slope failure scale type based on the 15-m grid-sized area.

slope-facing direction.

### 3.2 Occurrence and Scale of Slope Failures VS. Rainfall Indices

Fig. 5 shows the spatial frequency of slope failures for total precipitation  $F_{tp}$  for each slope failure scale type based on the 350-m grid-sized area. In southern Hiroshima Prefecture, as total precipitation increases, the frequency of slope failure increases significantly. Incidentally, the frequency of slope failure for total precipitation range of 200–250 mm is relatively high because of the occurrence of slope failure in the limited small area. The special local land factor in the area may influence their occurrence and this should be investigated in future works. The frequency of slope failure is high (> 10%) when total precipitation exceeds 450 mm, except the range of 200–250 mm. This is confirmed by overlapping of the high-density area of slope failure with the high total precipitation area in southern Hiroshima Prefecture (Fig. 6). However, in southeastern Ehime Prefecture, total precipitation and the frequency of slope failure are not correlated relatively.

Fig. 7 shows the spatial frequency of slope failure for maximum hourly precipitation  $F_{hp}$  for each slope failure scale type based on the 350-m grid-sized area. As maximum hourly precipitation increases, the frequency of slope failures increases in both study areas. Especially in southeastern Ehime Prefecture, the frequency of slope failures is high (> 20%) when maximum hourly precipitation

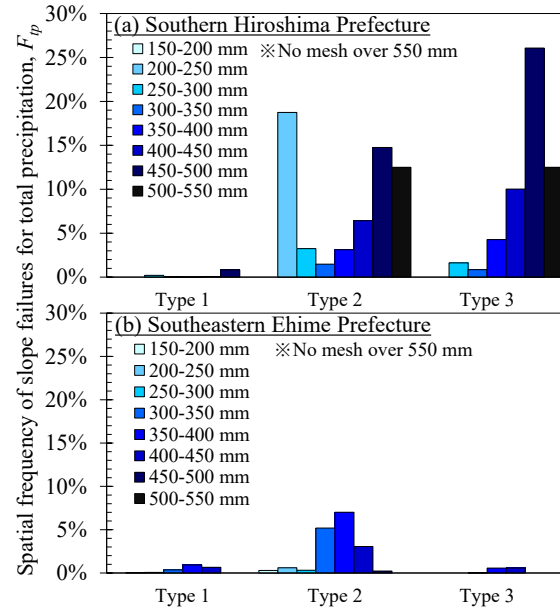


Fig. 5 Spatial frequency of slope failures for total precipitation ( $F_{tp}$ ) for each slope failure scale type based on the 350-m grid-sized area.

exceeds 80 mm. This is confirmed by overlapping of the high-density area of slope failure with the high maximum hourly precipitation area in southeastern Ehime Prefecture (Fig. 8).

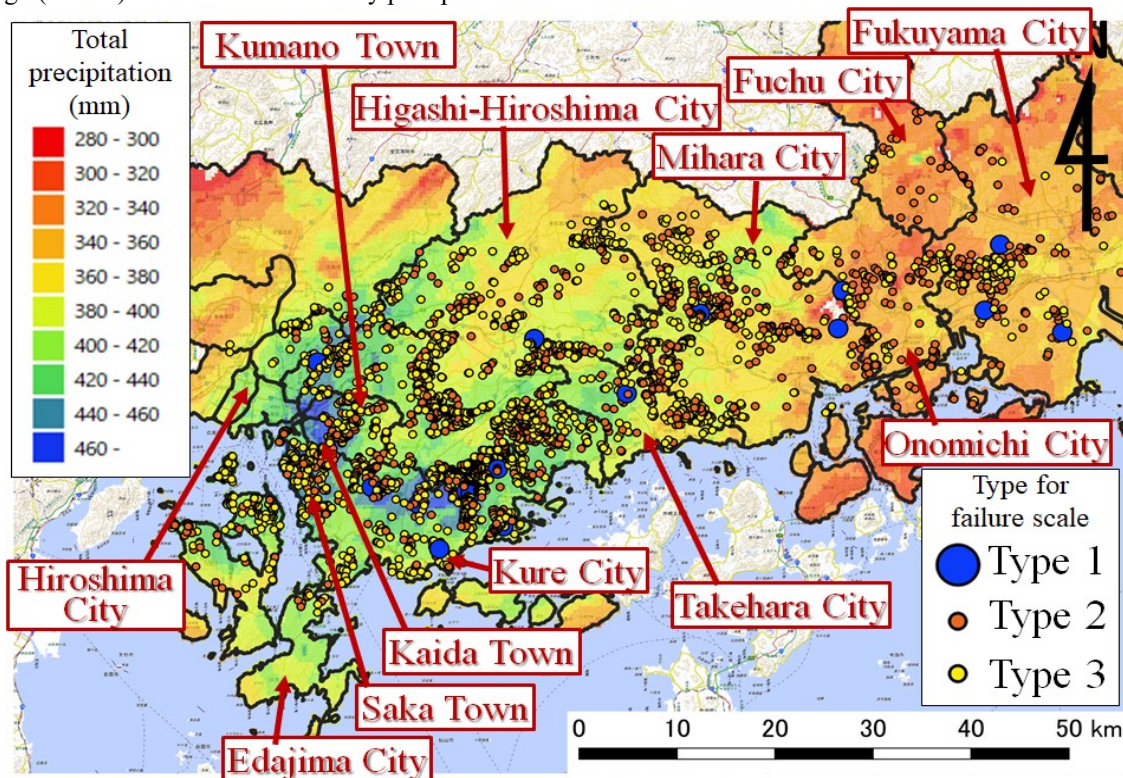


Fig. 6 Spatial distribution of slope failures for each slope failure scale type and total precipitation in southern Hiroshima Prefecture.

These results indicate that the occurrence and scale of typical slope failures depend on the rainfall indices with a different manner in each study area. Total precipitation (i.e., long-term rainfall index) is predominantly responsible for slope failure in southern Hiroshima Prefecture, whereas maximum hourly precipitation (i.e., short-term rainfall index) affects slope failure in both study areas. The study results also show that the 350-m grid-sized XRAIN data for the rainfall indices lead to a high possibility of estimating the occurrence of slope failure in the grid-sized area.

### 3.3 Occurrence of Slope Failures and Combined Indices of Local Land Factors and Meteorological Triggers

Table 2 shows the spatial frequency matrix of slope failures for all slope failure scale types and the combined indices of local land factors and meteorological triggers based on the 15-m grid-sized area. Using all 15-m grid DEM data without narrowing by any rainfall indices, the maximum spatial frequencies of slope failures for each slope gradients ( $F_{gr}$ ) in both study areas equal only 0.046% and 0.017%, respectively. However, as the lower limit of the maximum hourly and the total

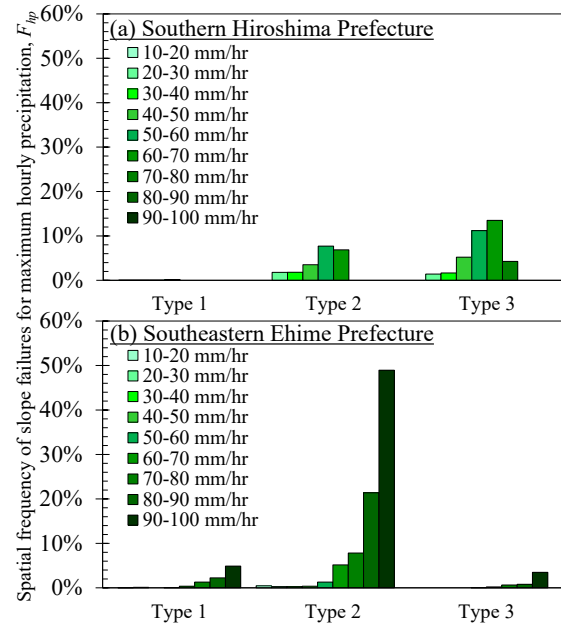


Fig. 7 Spatial frequency of slope failures for maximum hourly precipitation ( $F_{hp}$ ) for each slope failure scale type based on the 350-m grid-sized area.

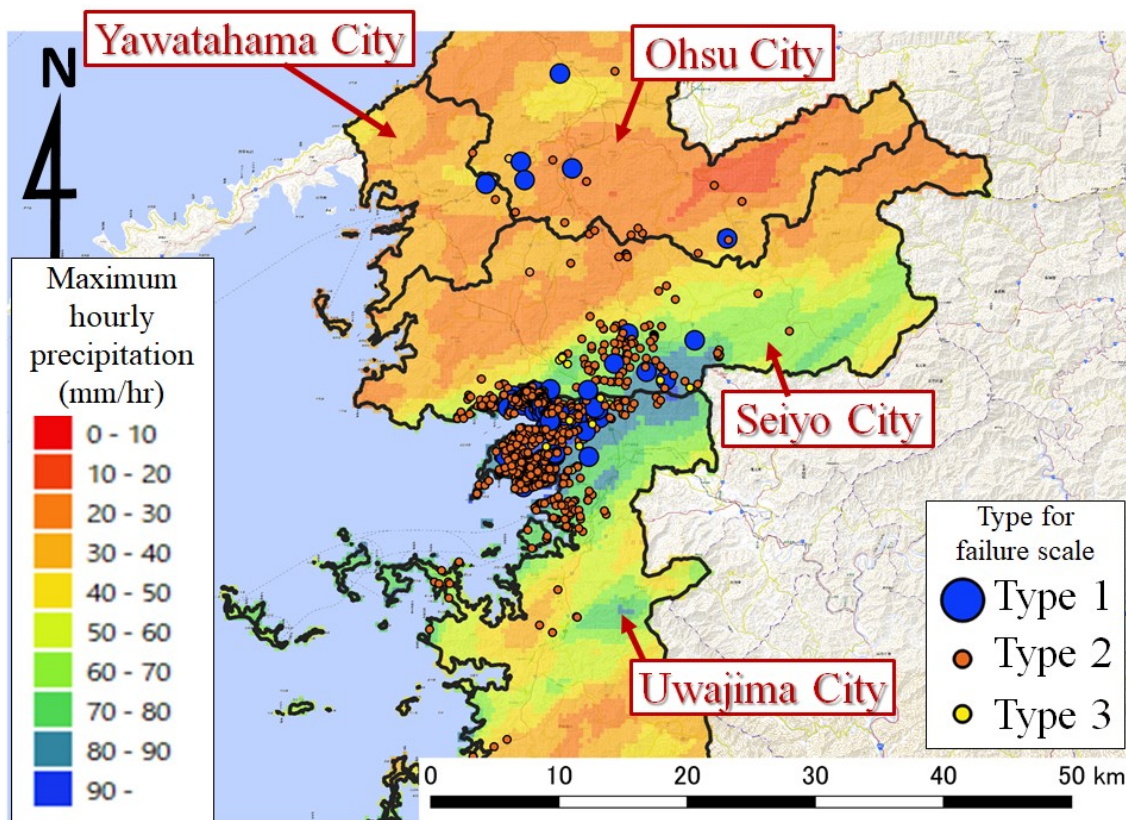


Fig. 8 Spatial distribution of slope failures for each slope failure scale type and maximum hourly precipitation in southeastern Ehime Prefecture.

Table 2 Spatial frequency matrix of slope failures for all slope failure scale types for a slope gradient and rainfall indices. The purple, red, orange, yellow and cream cell colors equal > 0.3%, > 0.2%, > 0.1%, > 0.05% and > 0.01%.

Slope gradient \ Rainfall index		Southern Hiroshima Prefecture					Southeastern Ehime Prefecture						
		0°- 10°	10°- 20°	20°- 30°	30°- 40°	40°- 50°	50°- 60°	0°- 10°	10°- 20°	20°- 30°	30°- 40°	40°- 50°	50°- 60°
Total precipitation	All data (Over 0 mm)	0.0026%	0.0179%	0.0459%	0.0382%	0.0131%	0.0186%	0.0007%	0.0045%	0.0096%	0.0163%	0.0167%	0.0034%
	Over 300 mm	0.0026%	0.0180%	0.0465%	0.0386%	0.0132%	0.0189%	0.0011%	0.0082%	0.0182%	0.0297%	0.0297%	0.0071%
	Over 400 mm	0.0037%	0.0404%	0.1027%	0.1002%	0.0512%	0.0565%	0.0014%	0.0032%	0.0075%	0.0102%	0.0133%	0.0000%
	Over 450 mm	0.0043%	0.0732%	0.1888%	0.2490%	0.1928%	0.0000%	0.0000%	0.0000%	0.0010%	0.0000%	0.0000%	0.0000%
Maximum hourly precipitation	All data (Over 0 mm/hr)	0.0026%	0.0179%	0.0459%	0.0382%	0.0131%	0.0186%	0.0007%	0.0045%	0.0096%	0.0163%	0.0167%	0.0034%
	Over 30 mm/hr	0.0029%	0.0214%	0.0561%	0.0489%	0.0181%	0.0203%	0.0031%	0.0184%	0.0389%	0.0629%	0.0602%	0.0127%
	Over 60 mm/hr	0.0032%	0.0369%	0.0859%	0.1203%	0.0824%	0.1057%	0.0050%	0.0426%	0.1122%	0.1969%	0.1961%	0.0473%
	Over 90 mm/hr	No rainfall data						0.0186%	0.1392%	0.2255%	0.3060%	0.1517%	0.0000%

precipitation increase,  $F_{gr}$  for all slope gradients increases more in both study areas. In addition, the rainfall indices that influence  $F_{gr}$  remarkably are different in each study area. In southern Hiroshima Prefecture, when a slope gradient ranges between 30° and 40° and total precipitation is over 450 mm,  $F_{gr}$  equals 0.249%, which is approximately 6.5 times higher than that without narrowing by any rainfall indices. In southeastern area Ehime Prefecture, when the slope gradient ranges between 30° and 40° and maximum hourly precipitation is over 90 mm/hr,  $F_{gr}$  equals 0.306%, which is approximately 18 times higher than that without narrowing by any rainfall indices. As a result, combining the topographic and rainfall indices may lead to a highly accurate estimation of the occurrence of slope failure on a smaller grid size than the unit size for the current system.

**4. CONCLUSION**

In this study, by using high-resolution data obtained from two areas in Japan, the spatial characteristics of the topographic and rainfall indices influencing the occurrence and scale of multiple slope failures in areas with smaller grid sized than the unit size for the current emergency alert system for sediment disasters in Japan are investigated.

The occurrence and scale of typical slope failures depend on a slope gradient and total precipitation (i.e., long-term rainfall index) with different relationship in each study area. Therefore, slope failures can be influenced by other factors, such as geological features. Whereas maximum hourly precipitation (i.e., short-term rainfall index) affects slope failure in both study areas.

The relationship between the spatial frequency of slope failure for all slope failure scale types and combining the topographic and rainfall indices,

which influence the occurrence and scale of slope failure, were investigated. The results indicate that there is a high possibility to estimate the occurrence of slope failure by combining these indices using a smaller grid size than the unit size for the current system.

Geological features and land use conditions were not considered herein. Therefore, it is necessary to evaluate the spatial frequency of slope failure based on these indices in both study areas in a future project. It is also essential to investigate the influence of the topographic and rainfall indices on the run-out distance of slope failure and the time interval from starting rainfall to an occurrence of slope failure (i.e., saturation time). It is also essential to estimate the influence of temporal changes in the short-term and long-term rainfall indices on the occurrence of slope failure. Furthermore, the proposed methodology has to be verified by applying it to other multiple slope failures.

**5. ACKNOWLEDGMENTS**

The field survey results used in this study is provided by the survey group of Japan Society of Erosion Control Engineering for the sediment disaster in Shikoku region caused by “Heavy Rain Event of July 2018”. The XRAIN dataset used in this study is provided by the Ministry of Land, Infrastructure, Transport and Tourism (MLIT) of Japan, and this dataset is archived and provided under the framework of the Data Integration and Analysis System (DIAS) funded by Ministry of Education, Culture, Sports, Science and Technology (MEXT) of Japan.

**6. REFERENCES**

[1] Kaibori M., Hasegawa Y., Yamashita Y., Sakida H., Nakai S., Kuwada S., Hiramatsu S.,

- Jitousono T., Irasawa M., Shimizu O., Imaizumi F., Nakatani K., Kashiwabara Y., Kato N., Torita E., Hirakawa Y., Yoshinaga S., Tanaka K. and Hayashi S., Sediment related disaster due to heavy rainfall in Hiroshima Prefecture in July, 2018, *Journal of the Japan Society of Erosion Control Engineering*, Vol.71, No.4, 2018, pp. 49-60. (in Japanese with English abstract)
- [2] Sasahara K., Ikeda T., Iwai Y., Kakuta K., Kanazawa A., Gonda Y., Saitou Y., Shuin Y., Tagata S., Fujita M., Miyata S., Miwa H., Murata I., Yamanoi K. and Wada T., Sediment Disasters in Shikoku Region in July, 2018, *Journal of the Japan Society of Erosion Control Engineering*, Vol.71, No.5, 2019, pp. 43-53. (in Japanese with English abstract)
- [3] Examination Committee for Enhancing a Workable Early Warning System for Sediment Disaster Reduction, The Sediment Disaster Report Caused by “Heavy Rain Event of July 2018” (Additional Document), 2018, p. 4. (in Japanese)
- [4] Wieczorek G. F., Landslides triggering mechanisms, In: Turner K. and Schuster R. L. (Eds.), *Landslides: Investigation and Mitigation*, National Research Council, Transportation Research Board, Washington, 1996, pp. 76–90.
- [5] Trigo R. M., Zêzere J. L., Rodrigues M. L. and Trigo I. F., The Influence of the North Atlantic Oscillation on Rainfall Triggering of Landslides near Lisbon, *Natural Hazards*, Vol.36, 2005, pp. 331–354.
- [6] Wieczorek G. F. and Glade T., Climatic Factors Influencing Occurrence of Debris Flows, In: Jakob, M. and Hunger, O. (Eds.), *Debris-flow Hazards and Related Phenomena*, Praxis, Springer, Berlin, 2005, pp. 325–362.
- [7] Guzzetti F., Peruccacci S., Rossi N. and Stark C. P., The Rainfall Intensity–Duration Control of Shallow Landslides and Debris Flows: an Update, *Landslides*, Vol. 5, 2008, pp. 3–17
- [8] Osanai, N., Shimizu, T., Kuramoto, K., Kojima, S., and Noro, T. (2010): Japanese early-warning for debris flows and slope failures using rainfall indices with Radial Basis Function Network, *Landslides*, Vol. 7, pp. 325–338
- [9] Yamagishi H., Saito M. and Iwahashi J., The Characteristics of the Heavy Rainfall-included Landslides in Izumozaki Area, Niigata, Japan – GIS Using Comparison Between 2004 July Failures and the Past Ones–, *Journal of the Japan Landslide Society*, Vol.45, No.1, 2008, pp. 57–63. (in Japanese with English abstract)
- [10] Iwahashi J., Yamagishi H., Kamiya I. and Sato H., Discriminant Analysis for Landslides Caused by the 2004 Niigata Heavy Rainfall in July and the Mid Niigata Prefecture Earthquake in October, *Journal of the Japan Landslide Society*, Vol.45, No.1, 2008, pp. 1-12. (in Japanese with English abstract)
- [11] Tanouchi H., Fujita S. and Egusa N., An Analysis of Endogenous Factors for Slope Failures Caused by 7.18 Flood Disaster in 1953, *Proceedings of the 9th Symposium on Sediment Disasters*, 2018, pp. 13–18. (in Japanese)
- [12] Kuramoto K., Tetsuga H., Kikuchi H., Morikawa O., Monma K. and Furukawa K., A Study on a Method for Determining Critical Line Using Geomorphological Factors of Slope Failures During Heavy Rainfall, *Journal of Japan Society of Civil Engineers*, No.658, 2000, pp. 207–220. (in Japanese with English abstract).

---

Copyright © Int. J. of GEOMATE. All rights reserved, including the making of copies unless permission is obtained from the copyright proprietors.

---